ANL/ESD/TM-15/4

Process Development for Nanostructured Photovoltaics

Project Period: September 15, 2009 to December 31, 2013

Energy Systems Division

About Argonne National Laboratory
Argonne is a U.S. Department of Energy laboratory managed by UChicago Argonne, LLC under contract DE-AC02-06CH11357. The Laboratory's main facility is outside Chicago, at 9700 South Cass Avenue, Argonne, Illinois 60439. For information about Argonne and its pioneering science and technology programs, see www.anl.gov.

DOCUMENT AVAILABILITY

Online Access: U.S. Department of Energy (DOE) reports produced after 1991 and a growing number of pre-1991 documents are available free via DOE's SciTech Connect (http://www.osti.gov/scitech/)

Reports not in digital format may be purchased by the public from the National Technical Information Service (NTIS):
U.S. Department of Commerce National
Technical Information Service 5301
Shawnee Rd
Alexandria, VA 22312
www.ntis.gov
Phone: (800) 553-NTIS (6847) or (703) 605-6000
Fax: (703) 605-6900
Email: **orders@ntis.gov**

Reports not in digital format are available to DOE and DOE contractors from the Office of Scientific and Technical Information (OSTI):
U.S. Department of Energy
Office of Scientific and Technical Information
P.O. Box 62
Oak Ridge, TN 37831-0062
www.osti.gov
Phone: (865) 576-8401
Fax: (865) 576-5728
Email: **reports@osti.gov**

Disclaimer
This report was prepared as an account of work sponsored by an agency of the United States Government. Neither the United States Government nor any agency thereof, nor UChicago Argonne, LLC, nor any of their employees or officers, makes any warranty, express or implied, or assumes any legal liability or responsibility for the accuracy, completeness, or usefulness of any information, apparatus, product, or process disclosed, or represents that its use would not infringe privately owned rights. Reference herein to any specific commercial product, process, or service by trade name, trademark, manufacturer, or otherwise, does not necessarily constitute or imply its endorsement, recommendation, or favoring by the United States Government or any agency thereof. The views and opinions of document authors expressed herein do not necessarily state or reflect those of the United States Government or any agency thereof, Argonne National Laboratory, or UChicago Argonne, LLC.

FINAL REPORT

Project Title:	Process Development for Nanostructured Photovoltaics
Date of Report:	January 27, 2014
Recipient:	Argonne National Laboratory 9700 S. Cass Avenue Argonne, Illinois 60439
Project Number:	FWP 4902A CFO Project Code: 2004320 Project ID Number: ANL_NPV ID: 18970
Project Period:	September 15, 2009 to December 31, 2013
Subcontractors:	Northwestern University
Other Partners:	InnoSense, LLC Batterson Cross Zakin Venture Partners Bloo Solar, Inc. Lotus Leaf Coatings
Contact:	Jeffrey W. Elam, 630-252-3520, jelam@anl.gov
Project Team:	DOE-HQ: Joseph Renk, (412) 386-6406 Northwestern University: Joseph Hupp InnoSense, LLC: Uma Sampathkumaran Batterson Cross Zakin Venture Partners: Robert Cross

Table of Contents

1) Executive Summary 3

2) Comparison of Project Goals and Accomplishments 4

3) Summary of Project Activities 5
- Task 1 5
- Task 2 13
- Task 3 17
- Task 4 20
- Task 5 22

4) Accomplishments 23
- Publications 23
- Presentations 23
- Inventions 24
- Technologies/Techniques 25
- Instruments/Equipment 26
- Software 26
- Awards 27

1) Executive Summary:

Photovoltaic manufacturing is an emerging industry that promises a carbon-free, nearly limitless source of energy for our nation. However, the high-temperature manufacturing processes used for conventional silicon-based photovoltaics are extremely energy-intensive and expensive. This high cost imposes a critical barrier to the widespread implementation of photovoltaic technology. Argonne National Laboratory and its partners recently invented new methods for manufacturing nanostructured photovoltaic devices that allow dramatic savings in materials, process energy, and cost. These methods are based on atomic layer deposition, a thin film synthesis technique that has been commercialized for the mass production of semiconductor microelectronics. The goal of this project was to develop these low-cost fabrication methods for the high efficiency production of nanostructured photovoltaics, and to demonstrate these methods in solar cell manufacturing. We achieved this goal in two ways: 1) we demonstrated the benefits of these coatings in the laboratory by scaling-up the fabrication of low-cost dye sensitized solar cells; 2) we used our coating technology to reduce the manufacturing cost of solar cells under development by our industrial partners.

2) Comparison of Project Goals and Accomplishments:

Status: The table below lists the milestones (project goals) and the milestone completion dates. All project milestones were met. Detailed descriptions of project activities are given in Section 3, Summary of Project Activities.

.

Milestone Number	Brief Description	Milestone Completion Date				Progress Notes
		Original Planned	Revised Planned	Actual	Percent Complete	
1	**Optimize prototype photovoltaic device**	03/11		06/11	100	*Completed*
1a	synthesize thin film aerogel samples	12/10		12/10	100	*Completed*
1b	prepare TCO coatings	12/10		12/10	100	*Completed*
1c	prepare wide bandgap semiconductor coatings	12/10		12/10	100	*Completed*
1d	fabricate, characterize, and test 1cmx1cm photocells	03/11		06/11	100	*Completed*
2	**Fabricate, characterize, and test 5cmx5cm optimized photocells**	09/11		9/11	100	*Completed*
2a	fabricate 5cmx5cm optimized photocells	06/11		06/11	100	*Completed*
2b	characterize 5cmx5cm photocells	09/11		9/11	100	*Completed*
2c	test 5cmx5cm photocells	09/11		12/11	100	*Completed*
3	**Fabricate, characterize, and test 10cmx10cm optimized photocells**	03/12			90	*On Track*
3a	fabricate 10cmx10cm optimized photocells	12/11		2/12	100	*Completed*
3b	characterize 10cmx10cm photocells	03/12	5/12	6/12	100	*Completed*
3c	test 10cmx10cm photocells	03/12	8/13		100	*Delayed*
4	**Fabricate and test 9-photocell module**	09/12			100	*Completed*
4a	fabricate 9-photocell module	09/12	8/13		50	*Cancelled*
4b	test 9-photocell module	09/12	8/13		0	*Cancelled*
4c	Process commercial 3D PV devices using ALD technology	12/13		12/13	100	*Completed*
5	**Team meetings and project reporting**	09/12			100	*Completed*
5a	Team meetings	09/12	12/13	12/13	100	*Completed*
5b	Project Reporting	09/12	12/13	01/14	100	*Completed*

3) Summary of Project Activities

<u>Task 1: Optimize prototype photovoltaic device</u>

<u>Task 1a: synthesize thin film aerogel samples</u>

The project began with establishing the safety plan and equipment for preparing thin film aerogels and xerogels at Argonne before work commenced. These aerogels and xerogels were intended to serve as the nanoporous scaffold or template for manufacturing the nanostructured photovoltaics. The main aim of the process development at Argonne was to find a scalable route for fabricating thin film aerogels that substitute the drop-casting method used at Northwestern for making prototype solar cells, since the drop-casting is not readily scalable. We investigated both draw-down or doctor blading methods that can be easily ported to 5x5 cm, 10x10 cm, and larger substrates without affecting the microstructure of the aerogels. Additionally, we focused on implementing other processes described in the literature that do not require either work in an ethanol saturated globe box or the use of supercritical drying, the latter an important factor aimed at cost-reduction during scale-up. The strategy followed was to modify the surface termination of the aerogel by substituting the terminal hydroxides by alkyl and silyl radicals to reduce the surface tension and enhance the spring-back effect during the atmospheric pressure drying process.

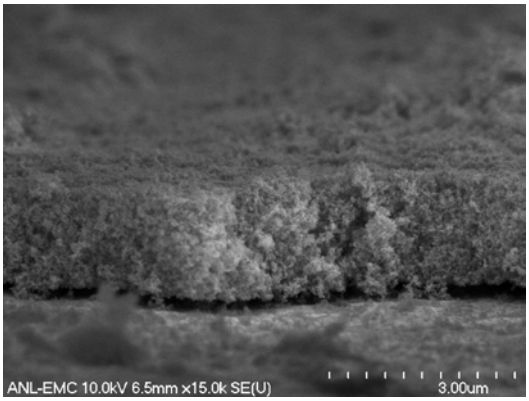

Figure 1: SEM image of Sb-doped SnO_2 film.

Argonne cast porous aerogel and xerogel thin films onto transparent conducting oxide (TCO) coated glass substrates. Argonne pursued a number of processes that were promising in terms of providing a surface area comparable to that of supercritically dried aerogels. Ambient pressure drying of surface functionalized aerogels and solvent exchange is a process that is well-described in the literature, and our work focused on achieving good adhesion to prevent delamination upon drying. The second process was based on the use of a functional scaffold which acts as the high-mobility core in a core-shell structure for fast electron transport.

Argonne optimized a low temperature processing route to fabricate highly conductive, porous Sb-doped SnO_2 (ATO) scaffolds. These scaffolds were cast in areas exceeding the 10x10 cm final milestone of the project. The films obtained were extremely uniform, and electrically connected without the need of carrying out an

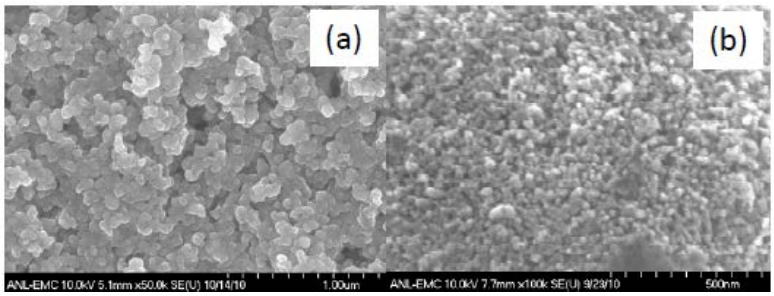

Figure 2: SEM images of: (a) 10 nm ALD TiO2 on ATO scaffold, (b) ZnO nanostructured electrode prepared using all-ALD route.

annealing procedure (Fig. 1). Sb-doped SnO_2 nanostructured substrates were cast using a drawdown method, and ALD of TiO_2 was performed to infiltrate the porous network (Fig. 2a). The resulting microstructures present a promising level of mesoporosity. Surface area and pore size distribution measurements were performed.

Argonne developed a new procedure for synthesizing ZnO nanostructured electrodes via a pure ALD route (Fig. 2b). Low temperature ALD on polymer nanosphere films followed by calcination leads to the formation of nanoporous substrates of similar microstructure as the conventional Graetzel TiO_2 electrodes. Two advantages of this approach are scalability and low processing time (hours vs. days when autoclaving is needed for the conventional particle synthesis). Argonne also identified a promising synthetic approach based on a two-step process using TEOS as starting the material that could lead to porous structures without the need for supercritical drying.

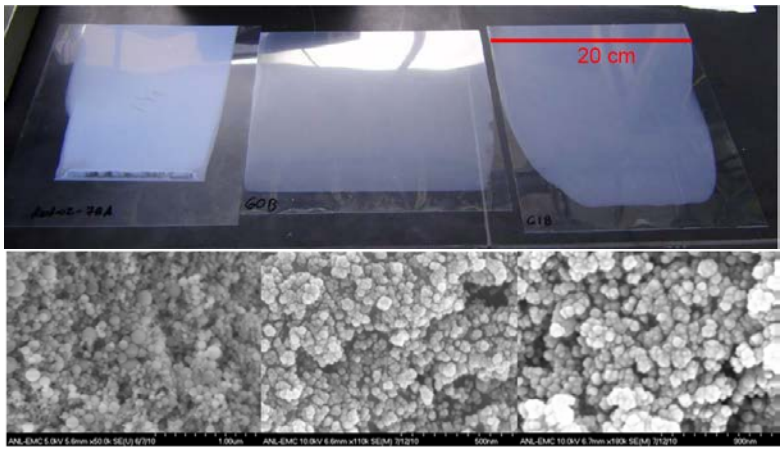

Figure 3: Scaffold samples prepared by thin-film drawdown. The first picture is an alumina scaffold that is approximately 50% porous. The second and third pictures are antimony tin oxide (ATO) scaffolds at approximately 50% porosity with 30% and 50% ATO content in the scaffold struts. SEM pictures of the samples are given below the respective films.

In addition to the aerogel and xerogel fabrication, particulate surface treatment studies were performed at Argonne in partnership with Batterson Cross Zakin Venture Partners. These materials were evaluated as an alternative substrate for the nanostructured photovoltaics that may allow lower cost manufacturing. the fabrication of aerogel-like conducting scaffolds using automated thin film drawdown. This is a lab method that simulates calendar coating or slot dye casting. Liquid formulations were spread on 8-in x 10-in PET sheets using a wire rod to control liquid film thickness. Film thickness was controlled by liquid film thickness and % solids in formulation. Scaffold samples are pictured in Fig. 3. The first picture is an alumina scaffold that is approximately 50% porous. The second and third pictures are Sb-doped tin oxide (ATO) scaffolds at approximately 50% porosity with 30% and 50% ATO content in the scaffold struts. SEM pictures of the samples are given below the respective films. The scaffolds were substantially transparent and the measured surface resistance is given in Figure 4 as a function of ATO loading.

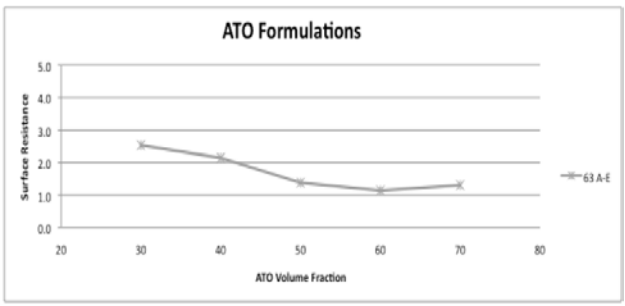

Figure 4: resistance of drawdown films versus ATO loading

As part of Task 1a, Innosense LLC (ISL) fabricated aerogels onto (0.5”x0.5”) fluorine-doped tin oxide (FTO)-coated substrates and delivered them to Argonne for ALD processing. ISL focused on improving aerogel synthesis using the conventional supercritical drying approach. ISL ordered and installed an E3100 Large Chamber Critical Point Dryer from EBSciences of East Granby, CT. The chamber has internal dimensions of 63.5 mm x 82 mm and equipped with a rupture disk rated for 1800 psi to ensure safe usage. Proof of concept experiments were conducted using Silbond 40 to synthesize monolithic aerogels. The Silbond 40 formulations consist of a mixture of Silbond 40 with 50 g of Silbond 40, 35 g of 200 proof ethanol, 14 g de-ionized water and 0.02 g HCl (30%). The contents were mixed at room temperature for 1 hour. A separate catalyst solution was then mixed containing 40 mL of 200 proof ethanol, 50 mL of de-ionized water, and 1.6 mL of ammonium hydroxide (30%). The final gel mixture was made by first combining 200 proof ethanol and Silbond 40 solution in a 1:1 volumetric ratio. To this mixture, the catalyst solution was slowly added in a final volumetric ratio of 1:20.

Figure 5: Silbond 40-coated FTO substrates for supercritical CO_2 processing.

ISL formulated silicate aerogel thin film coating structures for processing into solar cells using the supercritical carbon dioxide drying method. Using the above mentioned Silbond 40 formulations, gel-coated fluorine-doped tin oxide (FTO) substrates were typically loaded into a wire mesh (sample holder (Fig. 5). The holder was then filled with 20 mL ethanol for first few runs and the samples are submerged into the alcohol. The chamber was filled with liquid CO_2 from a CO_2 tank equipped with a siphon tube to a pressure of 800 psi at 15 °C. The chamber was then heated to 40 °C, giving a final drying pressure of approximately 1400 psi. Venting was performed over night with a depressurization rate of 100 psi/hr into water. The silicate aerogel thin film samples were then shipped to Argonne for infiltration using ALD AZO and TiO_2 layers and further processing into solar cells.

ISL also introduced polymeric scaffolds for use in dye-sensitized solar cells (DSSCs). Resorcinol–formaldehyde gels were adapted from protocols reported by Pekala and coworkers. Sols were initially drop cast onto clean fluorinated indium tin oxide (FTO) substrates. The samples were then baked for 3 days at 70 °C in a Barnstead/Lab-Line L-C oven to induce film gelation. After gelation, films were aged in an acid solution for 3 days followed by subsequent solvent exchange with acetone. Samples were then loaded into an E3100 supercritical reactor for drying. Polymeric gels exhibited higher apparent flexibility than similar silicate films. Figure 6 shows carbon aerogel thin films as dried in supercritical

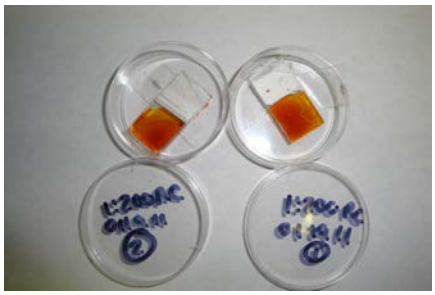

Figure 6. Carbon aerogel thin films.

conditions. Thus, there were fewer defects leading to film fracture. The porous polymer thin films were coated with TiO_2 through atomic layer deposition at Argonne National Laboratory.

ISL also developed low-density silicate and polymer scaffolds for TiO_2 and AZO coating via ALD. Supercritical drying was used to effectively remove production solvents from the gelled nanostructure to fabricate a highly porous network for coating. Previous samples were produced using ambient drying and silicate gels exclusively. These samples resulted in z-directed collapse, reducing available surface area that is accessible for TiO_2 coating due to evaporation-induced stresses. Supercritical drying greatly reduces phase change-induced stress that significantly affects film shrinkage and leads to structural defects. As a result, supercritically dried films offer higher porosity due to reductions in shrinkage during processing. Figure 7 shows the results after supercritical carbon dioxide drying is performed. These films did not reduce in thickness and offer excellent porosity as a result of water-dye testing at ISL. Water-dye testing was performed by placing a droplet of dyed water on the surface of the coating and observing the capillary phenomenon.

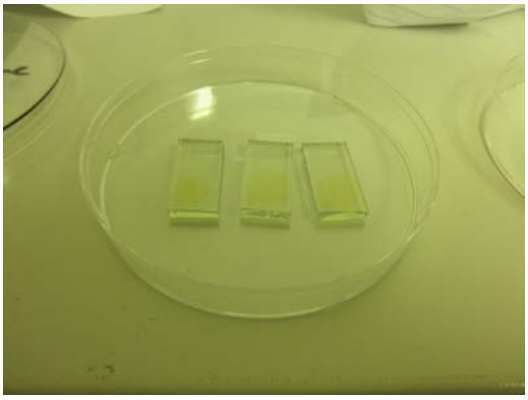

Figure 7. Silicate aerogel thin films after supercritical processing.

Process development also took place at Northwestern modifying the aerogel thin film method to reduce cracking and to allow thicker TiO_2 thin films, one of the most promising route to further boost the efficiency of dye sensitized solar cells. Northwestern optimized the process for aerogel synthesis to strengthen the porous network and improve the mechanical stability of the films.

Northwestern also invented methods for achieving broad spectral sensitization (i.e. light harvesting) to boost PV performance. Broad sensitization is essential for achieving high photocurrents and high energy-conversion efficiencies. Ideally one would like to collect photons over the wavelength range of 400 to ca. 800 nm (i.e. the entire visible spectrum and a portion of the near-infrared spectrum). This goal is difficult for any single dye to achieve and, consequently, several efforts have been made to co-sensitize photo-electrodes with complementary pairs of molecular dyes. Unfortunately, in addition to interacting photochemically with the electrode (a desired process), heterogeneous pairs of dyes often interact with each other, resulting in unproductive molecule-to-molecule electron transfer or hole-transfer.

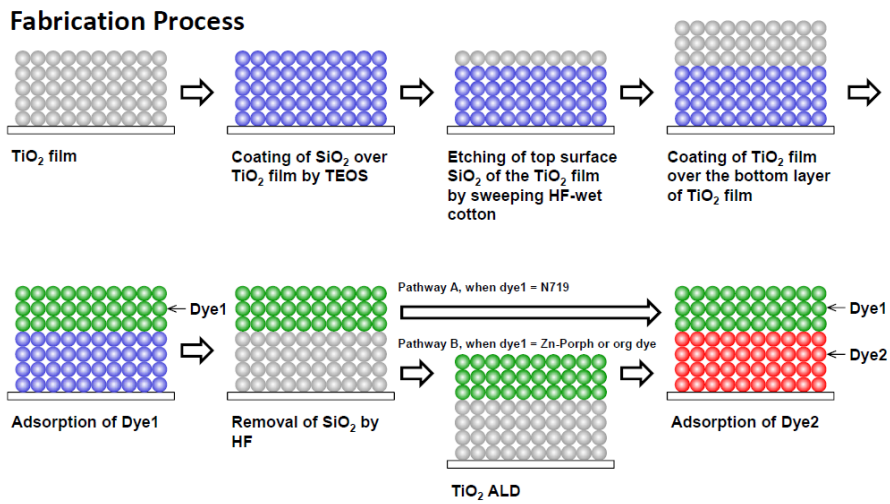

Figure 8: New strategy for 2-dye TiO_2 layer to achieve higher power conversion efficiencies by absorbing the full solar spectrum.

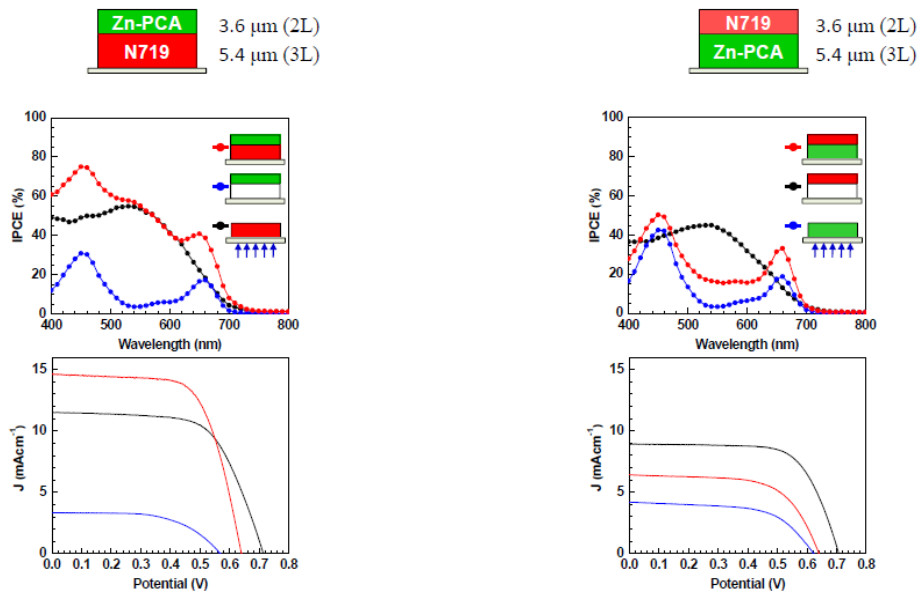

	J_{SC}	V_{OC}	FF	Eff.
N719+mpty	11.52	0.715	0.64	5.3
empty+ZnPCA	3.34	0.569	0.58	1.1
N719+ZnPCA	14.67	0.640	0.67	6.3

	J_{SC}	V_{OC}	FF	Eff.
ZnPCA+empty	4.18	0.622	0.60	1.6
empty+N719	8.91	0.708	0.69	4.3
ZnPCA+N719	6.43	0.641	0.63	2.6

Figure 9: Conventional dye N719, together with red-absorbing dyeZn-PCA, yield broader spectral absorption and higher power conversion efficiency.

Northwestern developed a method for completely circumventing dye-A/dye-B interaction problems. Briefly, they found that they could load dyes on photoelectrodes in stepwise fashion on separate layers of a high-area photoelectrode. The approach entails reversible electrode passivation and ALD-based enhancement of dye anchoring, among other processes. We find that dye co-sensitization of DSSCs indeed can be achieved. Additionally, by varying the loading order (dye-A → dye-B versus dye-B → dye A) they have been able to corroborate conclusions from other experiments that seemed to indicate, surprisingly, that electron-collection distances within DSSC photo-electrodes vary depending on the identity of the dye. These breakthroughs will allow for efficiency enhancements similar to those achieved in multijunction solar cells but with the advantage of using low temperature, low-cost processes. The key element of this approach is to spatially isolate the chromophores (Figure 8) and arrange the chromophores such that maximum advantage is taken of superior charge-collection behavior with one chromophore versus another. Previous work focused on sensitization pairs of organic chromophores. The new method utilizes the archetypal inorganic chromophore for dye-sensitized solar cells, N719, together with a complementary red-absorbing porphyrin chromophore, Zn-PCA. The net effect is that more of the solar spectrum is absorbed by the solar cell. This broader absorption results in greater photocurrent and therefore, greater overall light-to-electrical energy conversion efficiency (Figure 9)

<u>Task 1b: prepare TCO coatings</u>

This task focused on developing methods for depositing transparent conducting oxide (TCO) coatings. In particular, we developed ALD methods for depositing TCO films into the nanoporous thin film aerogel scaffolds from Task 1a, prepared at Argonne, Northwestern, and ISL. ALD excels at depositing highly uniform and conformal films inside of nanoporous materials such as thin film aerogels.

We developed a method for the ALD of In_2O_3 that uses a combination of H_2O and O_2 as the oxygen source. These two molecules act synergistically to produce the surface chemistry necessary for the In_2O_3 ALD – either compound alone is insufficient. The advantage of this method over previous methods for In_2O_3 ALD using O_3 as the oxygen source is that H_2O and O2 are both stable, unlike O_3 that can decompose on surfaces.

In addition, Argonne invented a new method to synthesize TCO thin films to obtain better electrical properties. This is based on adding a surface functionalization step that allows finer control over the spatial distribution of dopants in doped metal oxides. We optimized the growth of transparent conducting Al-doped ZnO films using this method. The effect of this process improves the conductivity of 10 nm AZO films by almost 50%. Argonne showed the scalability of this method and applied this process to the ALD of electron transport layers on top of Aerogel substrates provided by Innosense. These conductivity improvements were also obtained for Sn doped In2O3 transparent conducting oxides.

Argonne carried out ALD of ITO on Aerogel thin films supplied by Northwestern to study the influence of the work function of the electron transport layer on the performance and diffusion length of the electrons in the nanostructured devices.

Task 1c: prepare wide bandgap semiconductor coatings

Wide bandgap semiconductors, such as TiO_2, are integral to the nanostructured photovoltaic design as this component is responsible for creating and separating the photo-generated electron-hole pair that give rise to the photocurrent in the solar cell. In this task, Northwestern worked towards optimizing the wide bandgap semiconductors on the carrier collection efficiency on dye sensitized solar cells. Enhanced electron transport dynamics, diminished recombination dynamics, and enhanced porosity are three key issues to enhance the performance of the dye sensitized photovoltaic devices. The study of electron transport dynamics showed that transport is comparatively slow in TiO_2 aerogels, but roughly two orders of magnitude faster in ZnO aerogels. Unfortunately, the ZnO structures are susceptible to corrosion by functionalized dye molecules. TiO_2 aerogels, on the other hand, are chemically robust. We reasoned that robust structures displaying fast electron transport could be obtained by building coaxial aerogels comprising silica cores, ZnO shells, and outer protective layers of TiO_2. Experiments performed at Northwestern showed that these structures, which are fabricated by ALD, are indeed chemically robust. As shown in Fig. 10, they also display rapid electron transport.

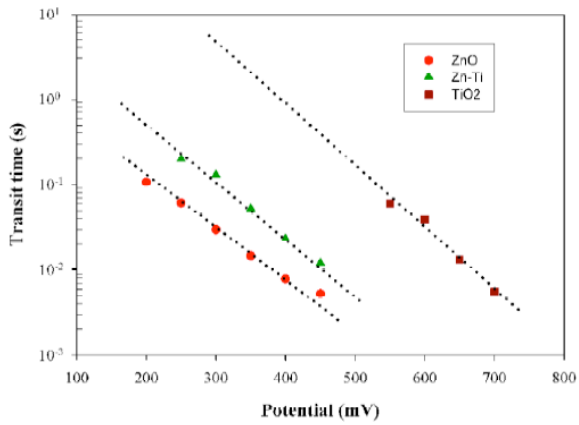

Figure 10. Transit time versus potential for ALD metal oxide materials.

Argonne optimized the deposition of TiO_2 on aerogels by two different ALD synthetic routes: using titanium tetrachloride and water and titanium tetraisopropoxide and water. We focused coating ATO nanoparticle substrates with TiO_2 at low temperatures, and determined the optical absorption of ATO/TiO_2/dye structures in order to optimize the optical properties of the nanostructured electrodes. We carried out TiO_2 growth on ITO/Aerogel scaffolds and measured the conformality of our multifunctional electrodes to optimize the process development. We also carried out growths of ZnO and TiO_2 thin films to form the core-shell structures studied by Northwestern. 5 nm, 10 nm and 15 nm thin films were grown in aerogels provided by ISL.

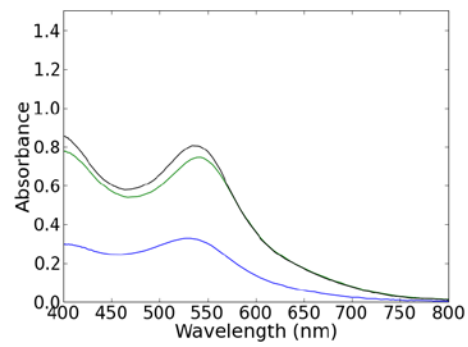

Figure 11: N719 absorbance on nanostructured electrodes of similar surface area: black - conventional NP; green - TiO_2 ALD annealed; blue - TiO_2 ALD as grown

Argonne also optimized the interfacial properties of TiO_2 thin films grown by ALD with the N719 dye. Optimal conditions were found in which the dye uptake per unit surface area is essentially the

same as that of conventional nanostructured electrodes based on anatase nanoparticles. Therefore, no efficiency losses are expected from poor dye uptake due to suboptimal interfacial quality (Fig. 11). Argonne also optimized the ALD process for both the growth of a protecting TiO_2 layer onto TCO/glass and Al foil substrates to reduce the shunting in the devices and for the overcoating of the nanostructured scaffolds

Task 1d: fabricate, characterize, and test 1cmx1cm photocells

Photovoltaic devices were fabricated and tested by Innosense, Northwestern, and Argonne. Aerogel thin films fabricated by Innosense and coated by ALD at Argonne were sent back to Innosense for further processing and testing. Photocells were assembled with TiO_2, ZnO/TiO_2, and AZO/TiO_2 photoanodes, and their performance evaluated. Figure 12 shows examples of these prototype nanostructured PV devices fabricated on both TCO/glass and foil substrates. To facilitate the PV evaluation, ISL acquired a Newport 150 W Solar Simulator Model 96000 fitted with a 1.5 A.M. filter and a beam turner to provide a constant irradiance source for photocell evaluation. Band pass filters for 520 nm and 650 nm wavelengths have also been purchased to evaluate wavelength specific photocell efficiencies. Figure 13 shows the results of evaluations performed for the prototype nanostructured PV devices, and the multiple curves in both graphs show measurements performed on different solar cells. The good agreement between these multiple measurements indicates the reproducibility of the fabrication and evaluation methods.

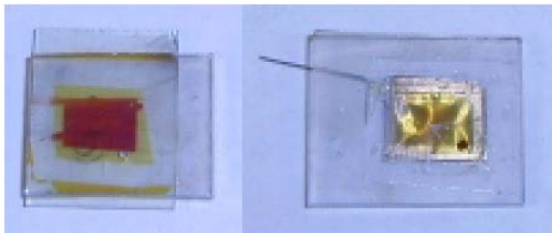

Figure 12: ALD core-shell nanostructured electrodes in TCO/glass and Al foil substrates.

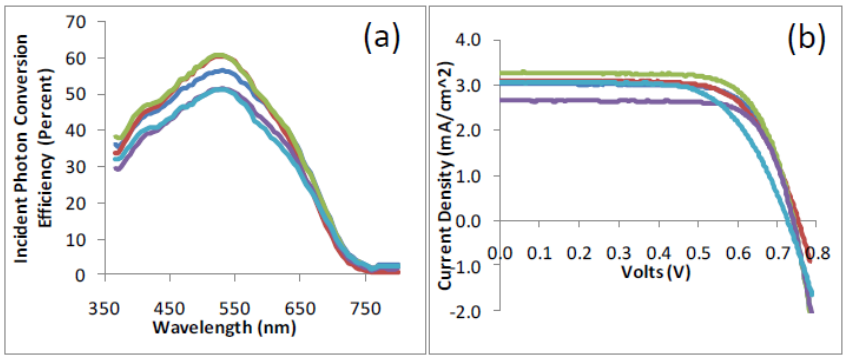

Figure 13: (a) Incident photon conversion efficiency versus wavelength, and (b) current density vs. voltage for ALD-modified DSSCs.

Two novel concepts were evaluated for the fabrication of the 1x1cm photocells:

1) The infiltrating hole-conducting polymers as a potential substitute for liquid electrolytes. We assembled mock solar cells based on this concept and explored different chemistries to improve the infiltration dynamics.

2) The use of ALD Pt catalyst in the cathode of the devices. The conventional drop casting approach for the Pt cathode presents a challenge for the scale up in terms of area homogeneity and ALD is a promising substitute for this process.

Although both concepts yielded working devices, the benefits were minimal and no further work was performed using these methods.

Northwestern University (NU) investigated the interplay between the kinetics and dynamics of electron collection, dye regeneration, regenerator diffusion, and (undesirable) interception of injected electrons by the oxidized form of the regenerator in determining the efficiencies of dye-sensitized solar cells. A weakness of the current best-performing cells is the use of the highly corrosive iodide/tri-iodide redox couple for regeneration. In addition to the challenges it presents with respect to cell stabilization, by spending ca. 0.55 V on the regeneration step the iodide/tri-iodide couple significantly degrades the open-circuit photovoltage and, therefore, the overall energy conversion efficiency. In principle, a more reactive regenerator would require much less than 0.55 V to regenerate the light absorber, and, therefore, could yield higher open-circuit photo-voltages. To be successful, however, this scheme would also require that the photo-electrode collect electrons faster as discussed above in Task 1a.

NU investigated the utility of cobalt-polypyridyl complexes as faster (and non-corrosive) regenerators. Previous studies of this class of regenerators have shown that they perform well at low light densities, but saturate at higher intensities. The problem has been traced to slow diffusion through conventional nanoparticulate photo-electrodes. The substantially greater porosity of aerogel-based photo-electrodes under development in this project should permit diffusion limitations to be overcome. In our brief investigation, we compared cells containing nanoparticulate, aerogel, and core-shell aerogel electrodes, with a cobalt couple being used as the dye regenerator. While the overall efficiencies of the best cells were comparatively low (ca. 2+%), the highly porous aerogel cells substantially outperformed the nanoparticulate cells. Additionally, we found that the core-shell aerogel-containing cells significantly outperformed the cells containing simpler aerogel photoelectrode structures. Overall, the efficiencies of aerogel core-shell type cells exceeded by roughly 12-fold the efficiencies of cells based on conventional nanoparticulate photoelectrodes. The combined results support the contention that core-shell aerogel architectures offer both superior molecular porosity and faster electron-collection kinetics.

Task 2: Fabricate, characterize, and test 5cmx5cm optimized photocells

Task 2a: fabricate 5cmx5cm optimized photocells

To facilitate the scale-up of the optimized nanostructured photovoltaics, it was necessary to incorporate a conductive grid on the transparent electrodes to enhance their current collection. Consequently, Argonne purchased a manual screen printer to deposit the silver grid and bus lines needed to reduce the series resistance of the larger area prototype. In addition, we identified an external supplier for custom drilled TCO glass substrates to carry out the cell filling for the 5x5 cm cells. Argonne fabricated dye sensitized solar cell prototypes with active areas greater than 5x5 cm. We successfully scaled-up the scaffold deposition, ALD growth, and cell

assembly using thermoplastic polymers as spacers and infiltrated the electrolyte using capillarity as the main driving force.

Argonne performed studies to optimize the formulation for the different nanoparticle substrates at the 5x5cm format. One of the challenges is to achieve a homogeneous thicknesses across different nanoparticle compositions to facilitate a meaningful comparison between the different core-shell architectures.

We developed different formulations based on fixed solid weight fractions on low-volatility solvents. We focused on 7.5% and 10% solid weight formulations. Ideally, using the same weight formulations would produce electrodes with the same thickness, but the rheological properties of the nanoparticle dispersion are strongly dependent on size and aspect ratio of the nanoparticles, and therefore it leads to different electrode thickness when applied using drawdown methods or screen printing.

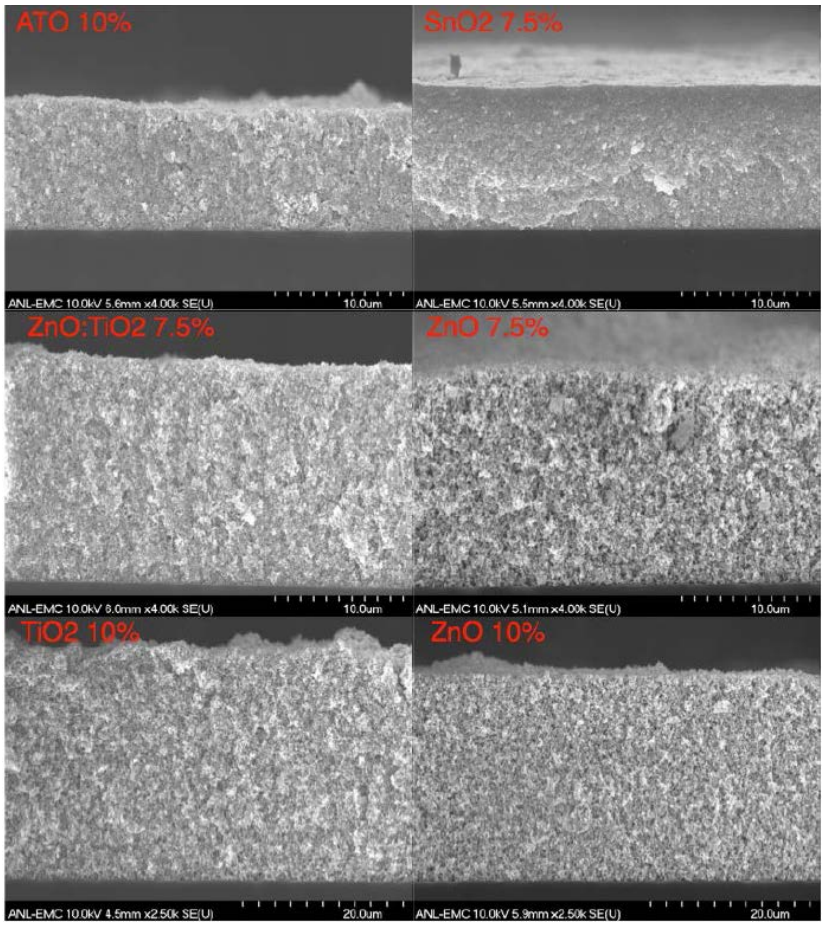

Figure 14: SEM images of nanostructured electrodes prepared by drawdown methods comprised of ZnO, TiO_2, ZnO/TiO_2, SnO_2, and Sb:SnO_2 scaffolds.

Figure 14 shows cross-section SEM images of nanostructured electrodes prepared by drawdown methods comprised of ZnO, TiO_2, ZnO/TiO_2, SnO_2, and Sb:SnO_2 scaffolds. We found that ZnO scaffolds are 50% thicker due to the higher viscosity of the dispersion even for the same weight percent. We also determined that ATO films are significantly thinner than the undoped counterparts. ZnO creates a much more open structures compared to the other scaffolds due to a larger particle size to produce a higher surface area which boosts performance.

Task 2b: characterize 5cmx5cm photocells

Larger PV devices demand that higher surface areas be coated during the ALD processing, and this can create new challenges that may affect the quality of the solar cells. To evaluate this possibility on the 5cmx5cm devices, we carrying out cross-section electron microscopy studies to determine the degree of infiltration of the ALD TiO_2 into the nanostructured electrodes for high area substrates. As shown in Fig. 15, we were able to identify experimental conditions that lead to good infiltration in large area substrates, producing high quality TiO_2/Sb:SnO_2 core-shell nanostructured electrodes.

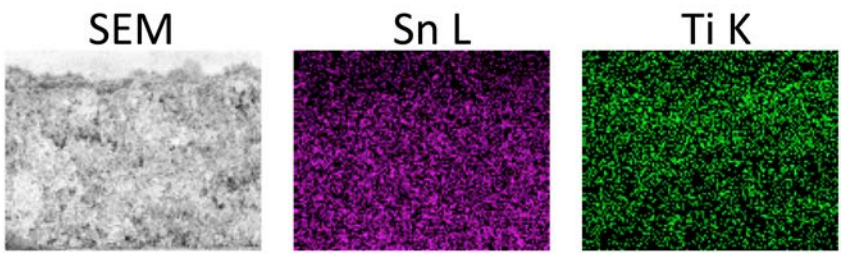

Figure 15: Cross Section SEM and elemental analysis of TiO_2/ Sb:SnO_2 core-shell nanostructured electrodes

We also examined the effects of electrode choice on the performance of the 5cmx5cm PV devices. Figure 16 compares the quantum efficiencies of Al_2O_3/TiO_2 and Sb:SnO_2/TiO_2 core shell nanostructured electrodes, showing that the effect of a conducting scaffold (i.e. the Sb:SnO_2) increases the maximum quantum efficiency by a relative 50%.

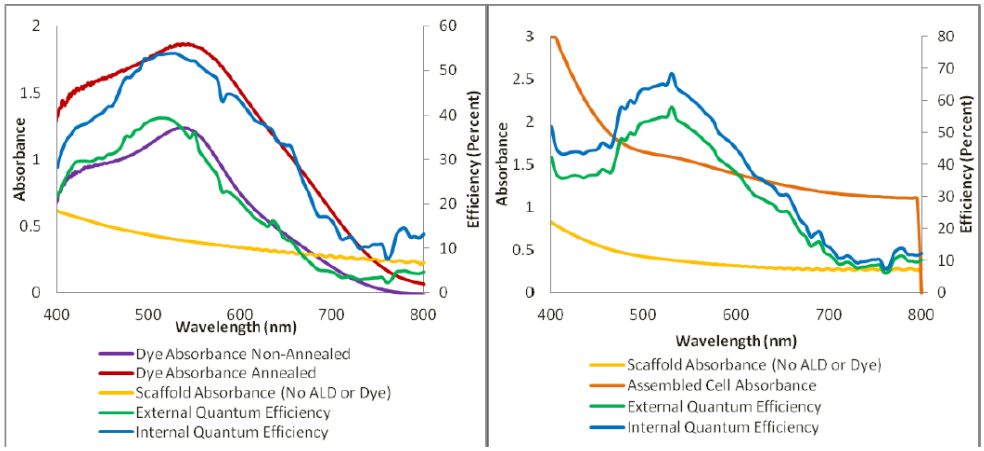

Figure 16: Comparison of the performance of AlO_3/TiO_2 (left) and Sb:SnO_2/TiO_2 (right) core shell nanostructured electrodes. Sb:SnO_2 core yields ~50% higher relative efficiency.

Task 2c: test 5cmx5cm photocells

We fabricated and tested 5cmx5cm nanostructured solar cells using the methodology established in Task 1 for the smaller, 1cmx1cm devices. We subjected them to the same range of tests to determine the short circuit current, open circuit voltage, fill-factor, and power efficiency. The results of these tests confirmed the successful scale-up from the 1cmx1cm to the 5cmx5cm format, since the performance was virtually the same. For instance, Fig. 17 shows a normalized current-voltage curve measured from a 5cmx5cm nanostructured solar cell prototype manufactured using the optimized core-shell architecture (ALD TiO_2 over ZnO nanoparticle scaffold) showing the exceptionally high open circuit voltage of ~ 1 V.

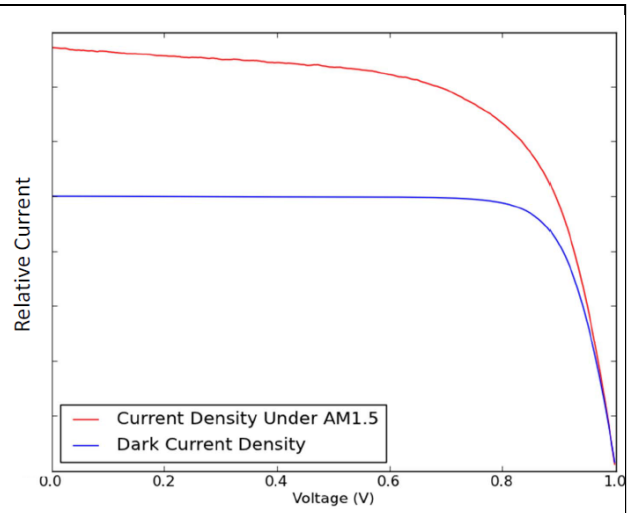

Figure 17: Current-voltage measurement of ZnO-TiO_2 core-shell nanostructured PV.

We carried out exhaustive testing of different oxide core/TiO_2 shell nanostructures at the 5cmx5cm format to isolate the impact that the different material combinations have in the efficiency, electron transport efficiency and optical properties of the photovoltaic devices. We prepared cells using TiO_2, ZnO, SnO_2, Sb:SnO_2 and Al_2O_3 cores using exactly the same cell assembly procedures. These cells underwent testing using spectroscopic impedance at Northwestern University to determine the impact that the core materials have on the characteristic diffusion length of the devices. We also tested their efficiencies under 1.5AM illumination using a large-area solar simulator. Figure 18 shows IV measurements for different Core/TiO_2 shell dye sensitized solar cells. All the nanostructured electrodes were prepared for a similar nominal thickness of 5 microns. The behavior can be grouped in two types: Sb:SnO_2 and SnO_2 present much larger open-circuit currents, but at the expense of lower fill factors and voltage potentials. The increase of short circuit current is consistent with a more efficient transport of electrons, which is one of the intended benefits of our approach. Note that this is more efficient for

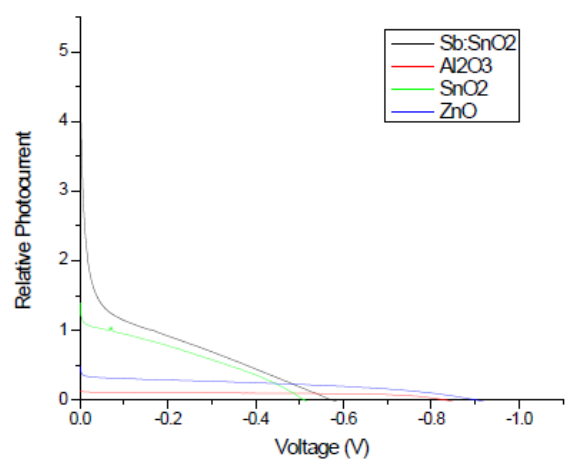

Figure 18: I-V curves of devices based on core-shell structured nanostructured electrodes for different core materials and a TiO2 shell.

the Sb-doped than for the intrinsic SnO_2. However, these cells have poorer fill-factors due to increased parallel resistance.

In the second type, ZnO and Al_2O_3, we have much better fill factors and greater open voltage potentials. In particular, the open voltage potential for the ZnO/TiO_2 is one of the largest reported in the literature. However, the photocurrents are two times smaller than that of the SnO_2 case. We believe that this is due to the larger particle size of ZnO scaffold (60-100 nm particle size distribution), which causes a much smaller surface area for the same thickness. Therefore, we believe that we can address this issue by moving to thicker cells. In contrast, the Al_2O_3 cell, which has an average particle size of just 40 nm, has an even smaller short circuit current, due to the inability of the electrons to travel through the core. This shows the advantages of having a conducting core (ZnO) vs. a passive one (Al_2O_3). From these results, we have selected ZnO and $Sb:SnO_2$ as the two candidates for the 10x10 cm^2 modules.

<u>Task 3: Fabricate, characterize, and test 10cmx10cm optimized photocells</u>

<u>Task 3a: fabricate 10cmx10cm optimized photocells</u>

We first acquired all of the necessary materials to perform screen printing of the silver electrodes for the larger, 10cmx10cm photocells. In addition, screen printing masks were designed and fabricated for optimal performance, to give the best compromise between low resistance and high optical transmission. The current collection grid and bus were optimized for application to both the anode and cathode of the device. This electrode design is shown in as shown in Fig. 19.

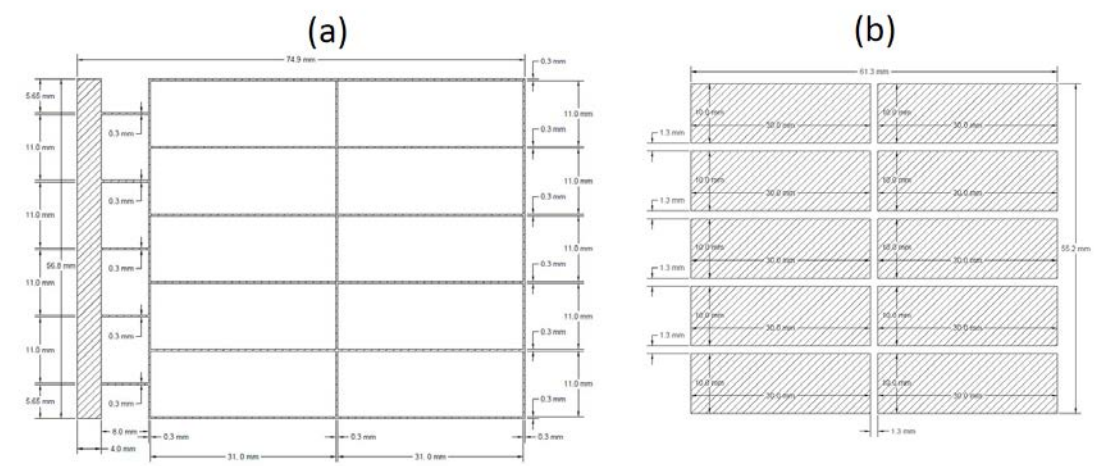

Figure 19: Silk screen patterns for Ag electrodes (a) and nanostructured scaffold (b).

Custom TCO glass parts were manufactured to allow the filling of the nanostructure. The design was based on a single cavity 10x10 cell that maximizes the active area and that has multiple holes for fast electrolyte filling. Figure 20 shows the silk-screening device with the mask installed, and also the resulting electrodes deposited on the custom TCO glass. The

silver patterned lines resulted in and electrode resistance across the device two orders of magnitude lower with respect to the value in the bare TCO glass. The screen printing of the Pt catalyst was also optimized using the design depicted in Fig. 19b.

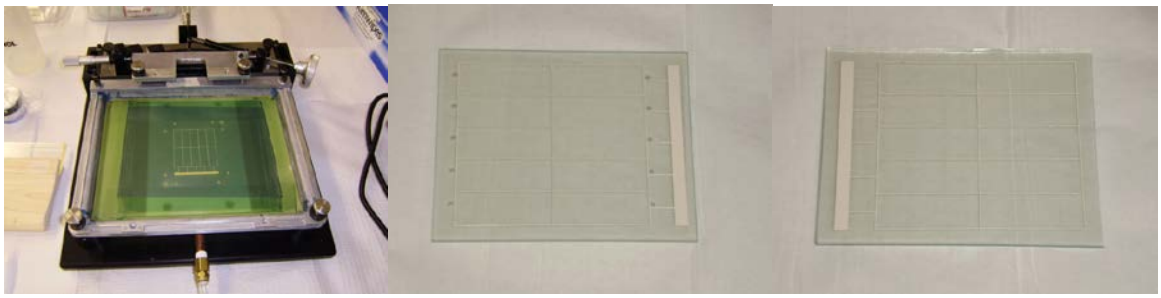

Figure 20: Silk screen mask and screen printed current collectors for a 10x10cm device.

We fabricated and characterized a number of 10x10cm nanostructured photovoltaic devices utilizing the silk screen printing facility and photomask. Figure 21 shows a completed 10x10cm photocell after screen printing of the porous scaffold, ALD treatment, infiltration of the organic dye, and finally infiltration of the electrolyte solution. As shown in Fig. 21, the dye loading is essentially homogenous over the entire 10x10 cm area.

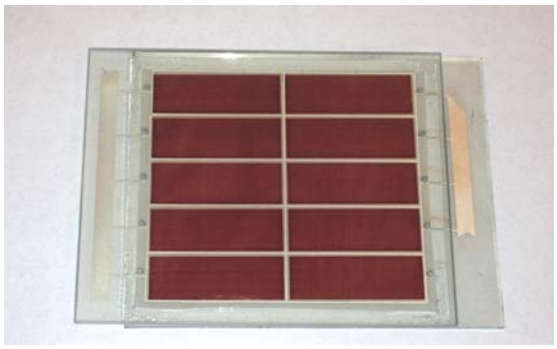

Figure 21: Completed 10x10cm nanostructured photovoltaic device incorporating these screen-printed current collectors.

We scaled up the synthesis of the screen printing ZnO and Sb:SnO_2 pastes based on low-volatility formulations up to 50 g batches. The new formulations were based on ethoxyethanol and butoxyethanol, which are widely available industrial solvents. They avoid the evaporation problems of the formulation prepared for the small-scale cells, based on volatile alcohol solvents. A photograph of the scaled-up paste is shown in Fig. 22, in comparison to the 10g batch of commercial TiO_2 paste obtained from Solaronix.

Figure 22: Comparison of our scale up nanoparticle paste (Sb:SnO2) and 10g batch TiO2 paste from Solaronix

Task 3b: characterize 10cmx10cm photocells

We encountered a problem with delamination of the silver contacts from the F-SnO_2 coated glass substrate. We discovered that this problem could be circumvented by adjusting the formulation of the silver screen printing paste.

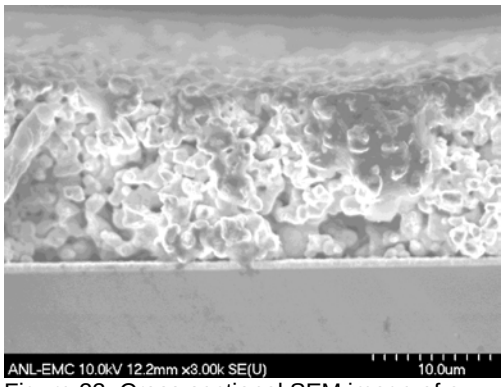

Figure 23: Cross sectional SEM image of a TiO2 coated silver trace on TCO glass.

An additional challenge encountered was that the silver bus lines needed to be protected to prevent oxidation during thermal treatment and corrosion by the electrolyte. To address this issue, we deposited and ALD TiO_2 overcoating layer on the silver contacts after the silk screening procedure. Cross sectional SEM characterization of the coated silver grids (Fig. 23) shows the presence of an ALD overcoating that not only protects the surface, but effectively coats the internal pores of the screen printed layer, protecting the silver from the degrading action of the electrolyte. The advantage of this process is that it is carried out using the same system that is used for the coating of the ALD TiO_2 shells and the underlying TiO_2 layers on the TCO.

Task 3c: test 10cmx10cm photocells

Initial testing of the 10x10 cm cells with the optimized fabrication procedure revealed a low parallel resistance consistent with the presence of a short circuit, even after solving the aforementioned delamination issue. We identified the overlap of the photoanode and photocathode silver meshes as the root cause. We modified the design of the silver grids to have an interdigitated structure as shown in Fig. 24, which avoids this overlap by eliminating the lines parallel to the thick silver bus.

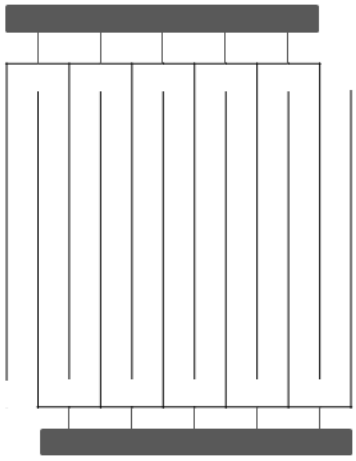
Figure 24: New interdigitated design that avoids overlap between silver the photocathode and photoanode silver mesh

Task 4: Fabricate and test 9-photocell module

Task 4a: fabricate 9-photocell module

We planned our assembly of the 9-photocell module based on our definitive design of the 10x10 cm photocell using one large silver bus as the main current collector (Figure 25). We designed a 3x3 module based on a series connection of the devices that should lead to a module providing open circuit voltages around 6V. As shown in Figure 25, our design incorporated silver bus lines as connection points to assemble rows of three photocells connected in series. Rows are then connected through a single conducting path to their neighbors, and otherwise will be electrically isolated from each other in order to prevent short circuiting of the series connection.

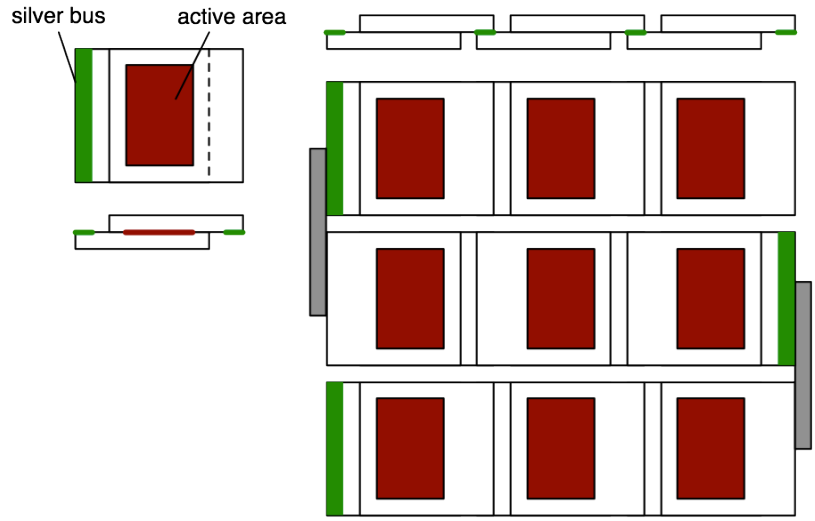

Figure 25: Design of the 3x3 photocell module based on a series connection configuration. Expected Voc: 6 V.

Task 4b: test 9-photocell module

Cancelled: As a consequence of a promising partnership with Bloo Solar Inc. that began in 2012 Q2 to develop ALD technology for their 3D PV devices, we elected to devote the remaining time and funding to this industry project. Therefore, we cancelled Task 4b, and Initiated Task 4c.

Task 4c: Process commercial 3D PV devices using ALD technology

In 2012 Q2 we engaged three companies interested in evaluating the ALD technology developed in this project for potential licensing. Lotus Leaf Coatings, Bloo Solar, and First Solar. After discussions, we signed agreements with two of the companies. Lotus Leaf Coatings (Albuquerque, NM) manufactures and distributes proprietary superhydrophilic and superhydrophobic coatings for optics, micro-electronics, fluid dynamics, anti-fogging and other applications. These superhydrophilic and superhydrophobic coatings are based on silica aerogels which are a nanoporous form of glass. Lotus Leaf Coatings wanted to evaluate the benefit of ultrathin, conformal films on the mechanical and structural properties of their coatings. Through this nanomanufacturing project, Argonne developed unique expertise and facilities for

depositing films inside of nanoporous and nanostructured materials such as silica aerogels using atomic layer deposition (ALD). We signed a Technical Service Agreement to coat substrates supplied by Lotus Leaf Coatings with ALD films and return them to Lotus Leaf Coatings for their evaluation. We coated coupons for Lotus Leaf and they measured the physical properties of these coated coupons to determine whether our ALD coatings are suitable for their superhydrophilic and superhydrophobic products.

Bloo Solar, Inc., (El Dorado Hills, CA) designs, develops and manufactures solar photovoltaic (PV) modules. Bloo Solar is a third generation solar technology that is designed to optimize PV performance by converting more of the sunlight that strikes our modules into electricity utilizing a novel three-dimensional substrate structure. In the course of this nanomanufacturing project, Argonne invented technologies for coating three-dimensional substrates with transparent conducting oxide (TCO) layers based on atomic layer deposition (ALD). Argonne has signed a Work for Others Agreement with Bloo Solar to coat their substrates with ALD TCO layers and return them to Bloo Solar for their evaluation. We deposited ALD ITO and ZnO on coupons and returned them to Bloo Solar. Based on promising results, we proceeded to coat their 3D PV devices. Bloo Solar determined that the performance of the ALD coatings was superior to that of conventional sputtered coatings.

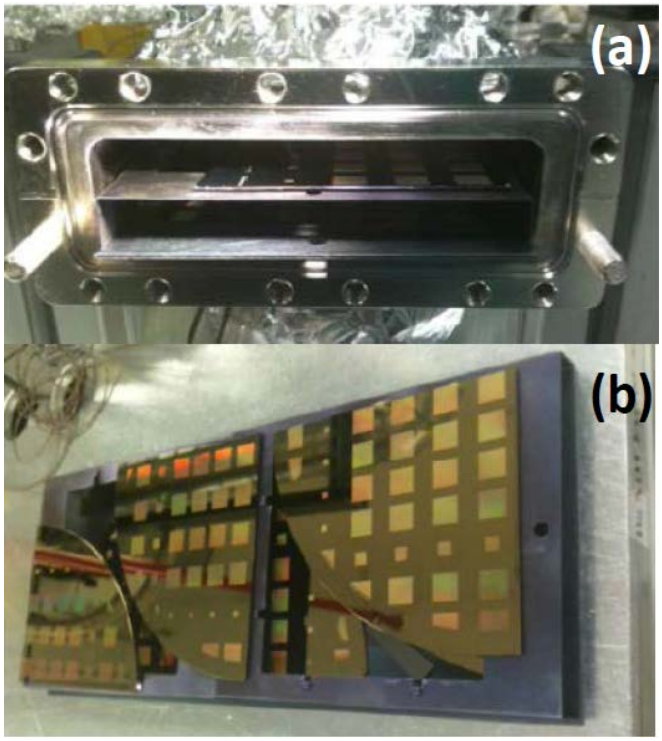

Figure 26: (a) Entry of new large area reactor, (b) ALD Al-ZnO transparent conducting oxide films deposited on multiple, 4" substrates of prototype 3D PV devices.

Next, we carried out the deposition of ITO and ZnO on large area substrates and nanostructured photovoltaic devices provided by Bloo Solar, achieving less than 3% variation across a 30 cm distance and 2% run-to-run variations. A double-deck substrate holder further increased our ability to coat simultaneously multiple nanostructured devices. Figure 26 shows an example of nanostructured PV devices after being coated inside of the large area reactor. These PV devices are currently being evaluated by Bloo Solar. Based on the results of these evaluations, we intend to establish a CRADA with Bloo Solar to facilitate the technology transfer.

Task 5: Team meetings and project reporting

Task 5a: Team meetings

Conference calls were held between Innosense and Argonne to coordinate the sample exchanges and to plan the next iteration cycle of their thin film aerogel fabrication process. Coordination between Argonne and Northwestern was done with face-to-face visits given the close proximity of the two institutions. Argonne personnel visited Northwestern to evaluate solar cell fabrication methods, and also Northwestern personnel visited Argonne to evaluate ALD facility and receive training to become regular users of our experimental system. Weekly group meetings at Argonne and Northwestern were held to review progress.

Task 5b: Project Reporting

Quarterly progress reports, and a final report, were prepared and submitted to DOE as required by the program.

4) Accomplishments:

Publications:

1) Yanguas-Gil, J. A. Libera, and J. W. Elam, "Modulation of the growth per cycle in Atomic Layer Deposition using reversible surface functionalization", Chemistry of Materials **25**, 4849-4860, (2013). doi: dx.doi.org/10.1021/cm4029098
2) Yanguas-Gil, J. A. Libera, and J. W. Elam, "In-Situ FTIR Characterization of Growth Inhibition in Atomic Layer Deposition Using Surface Functionalization", ECS Transactions, 50 (13), 43-51, (2012).
3) Yanguas-Gil and J. W. Elam, "Simple model for atomic layer deposition precursor reaction and transport in a viscous-flow tubular reactor", J. Vac. Sci. Technol. A, 30 (1), 01A159-1-01A159-7, (2012).
4) Yanguas-Gil and J. W. Elam, "Self-limited reaction-diffusion in nanostructured substrates: surface coverage dynamics and analytic approximations to ALD saturation times", CVD, 18, 46-52 (2012).
5) Yanguas-Gil, and J. W. Elam, "Diffusion-Reaction Model of ALD in Nanostructured Substrates: Analytic Approximations to Dose Times as a Function of the Surface Reaction Probability", ECS Transactions, 41, (2), 169-174, (2011).
6) Yanguas-Gil and J. W. Elam, "Controlled dopant distribution and higher doping efficiencies by surface-functionalized atomic layer deposition", Chemistry of Materials, 23 (19), 4295-4297, (2011).
7) Yanguas-Gil and J. W. Elam, "Growth rate control in ALD by surface functionalization: alkyl alcohols on metal oxides", ECS Trans. 33 (2), 333 (2010).
8) D. Hess, M. Mushfiq, R. Dalvi, R. Winter, U. Sampathkumaran, K. Goswami, A. Yangaus-Gil, and J. W. Elam, "Dye-Sensitized Solar Cells Fabricated from Atomic Layer Deposited Photoanodes on Aerogel Scaffolds", ECS Trans. 33 (2), 245 (2010).

Presentations:

1) J. W. Elam, 13th International Conference on Atomic Layer Deposition, ALD2013, San Diego, CA, "ALD Process Selection for Scalable Nanomanufacturing", Contributed Talk, (July 30, 2013).
2) J. W. Elam, University of Wisconsin at Madison, Materials Science Program Seminar, Madison, WI, "Beyond A/B/A/B… Unorthodox Pulse Sequences in Atomic Layer Deposition", Invited Talk, (December 13, 2012).
3) J. W. Elam, University of Colorado, Materials & Nanoscience Seminar, Boulder, CO, "Atomic Layer Deposition for Nanomanufacturing", Invited Talk, (November 11, 2012).
4) J. W. Elam, NSC/ANL Workshop, Taipei, Taiwan, "Synthesis of Nanomaterials Using Atomic Layer Deposition", Invited Seminar, (January 12, 2012).
5) J. W. Elam, Nanomanufacturing Symposium, Eindhoven, Netherlands," Process Development and Scale-Up of Atomic Layer Deposition for Nanomanufacturing" , Invited Seminar, (May 11, 2012).
6) J. W. Elam, 35th International Conference on Advanced Ceramics and Composites, Daytona, FL, "Atomic Layer Deposition Synthesis of Nanostructured Coatings", Invited Seminar, (January 27, 2011).

7) J. W. Elam, Cambridge NanoTech ALD Spring Retreat 2011, Stanford, CA, "Atomic Layer Deposition Research at Argonne", Invited Seminar, (March 15, 2011).
8) J. W. Elam, University of Notre Dame Solid-State Seminar, Notre Dame, IN, "Atomic Layer Deposition Synthesis for Advanced Photovoltaics", Invited Seminar, (February 4, 2011).
9) J. W. Elam, TMS 2011 - 140th Annual Meeting, San Diego, CA, "Atomic Layer Deposition for the Functionalization of Nanoporous Materials", Invited Seminar, (March 1, 2011).
10) J. W. Elam, 11th International Conference on Atomic Layer Deposition, ALD2011, Boston, MA, "Indium Oxide Atomic Layer Deposition Facilitated by the Synergy between Oxygen and Water", Contributed Talk, (June 28, 2011).
11) Angel Yanguas-Gil and Jeffrey W. Elam, "Growth rate control in ALD by surface functionalization: alkyl alcohols on metal oxides", 10th International Conference on Atomic Layer Deposition, Seoul, Korea (2010).
12) Angel Yanguas-Gil and Jeffrey W. Elam, "Growth Rate Control in Atomic Layer Deposition by Surface Functionalization", 218th ECS Meeting, Las Vegas, NV (2010).
13) D. Hess, M. Mushfiq, R. Dalvi, R. Winter, U. Sampathkumaran, K. Goswami, A. Yangaus-Gil, and J. W. Elam, "Dye-Sensitized Solar Cells Fabricated from Atomic Layer Deposited Photoanodes on Aerogel Scaffolds", 218th ECS Meeting, Las Vegas, NV (2010).
14) Angel Yanguas-Gil and Jeffrey W. Elam, "Growth Rate Control in ALD by Surface Functionalization", AVS 57th International Symposium, Albuquerque, New Mexico (2010).
15) A. Yanguas-Gil, J. W. Elam, V. Williams, U. Sampathkumaran, M. J. Pellin, and J. T. Hupp, "Dye sensitized solar cells with aerogel-templated nanostructured photoanodes fabricated using Atomic Layer Deposition", AVS 57th International Symposium, Albuquerque, New Mexico (2010).
16) A. Yanguas-Gil and J. W. Elam, "ALD Growth per Cycle Modulation Using Surface Functionalization: A Strategy for Improved Stoichiometry Control and Higher Doping Efficiencies", 11th International Conference on Atomic Layer Deposition, Boston, MA (2011).
17) T. Martin, A. Yanguas-Gil, R. W. Brotzman, J. A. Libera, and J. W. Elam, "Nanostructured Photovoltaic Devices Based on ALD of Wide Bandgap Semiconductor and Transition Metal Oxides", 11th International Conference on Atomic Layer Deposition, Boston, MA (2011).

Inventions and Patents:

1) A. Yanguas-Gil, J. A. Libera, and J. W. Elam, "Method for continuous ALD", IN-13-042, (2013).
2) A. Yanguas-Gil and J. W. Elam, "Enhancement of materials and interface performance of materials via ALD infiltration", ANL- IN-11-088, (2011).
3) U. Mane and J. W. Elam, "Method for Producing Highly Conformal Transparent Conducting Oxide Films", ANL-IN-11-042, (2011).
4) R. Brotzman, A. Yanguas-Gil, T. Martin, and J. W. Elam, "DSSC Solar Cell", ANL-IN-11-047, (2011).

5) A. Yanguas-Gil and J. W. Elam, "Deposition Control in Porous Substrates using Surface Modification in Atomic Layer Deposition", ANL-IN-11-027, (2011).
6) A. Yanguas-Gil and J. W. Elam, "Growth Rate Control in ALD by Surface Functionalization", ANL- IN-10-028, US Patent Application 2012/0213946 A1, published August 23, 2012.
7) J. W. Elam and J. A. Libera, "Improved Method for Depositing Transparent Conducting Oxides", ANL-IN-09-080, US Patent Application US20110206846 A1, published August 25, 2011.
8) A. Yanguas-Gil, J. A. Libera, and J. W. Elam, "Method for continuous ALD", IN-13-042, (2013).

Technologies/Techniques

1) Surface Functionalization: We developed a methodology to modulate precursor-surface reactivity and tailor the growth per cycle in Atomic Layer Deposition. Our approach relies on in-situ surface functionalization to control the density of reactive sites on the growing surface using the sequential dosing of a surface inhibitor, the ALD precursor, and the co-reactant. We have demonstrated this methodology for ALD processes based on alkyl, cyclopentadienyl, halide, alkylamido, alkoxide, and beta-diketonate precursors, and a wide-range of inhibitors, including alkyl alcohols, ketones, carboxylic acids, and beta-diketones, in all cases resulting in a modulation of the growth per cycle due to the presence of functional groups on the surface. The utility of this surface functionalization technique is that this can be used to optimize the distribution of dopants in a lattice to improve the properties of a material. For instance, using surface functionalization we successfully increased the doping efficiency of Al in Al-doped ZnO films by 2x. Al-doped ZnO is a candidate transparent conducting oxide for next-generation photovoltaics, and our surface functionalization technique can be used to enhance the conductivity of these films, so that a thinner film can be used, and ultimately lower the manufacturing costs of these devices.

2) ALD of Transparent Conducting Oxides using TMIn: An improved method and system for producing indium oxide (In_2O_3) and other transparent conducting oxides was devised. In_2O_3 can also be doped with tin to form indium tin oxide ("ITO") with improved electrical conductivity, high optical transparency and good chemical stability. Deposition of such materials is accomplished by using atomic layer deposition ("ALD") to deposit ITO (and other such transparent conducting oxides) over large areas with high uniformity to address selected commercial applications. The ALD method is used in conjunction with particular precursor materials, such as trimethyl indium (TMIn") due to its high vapor pressure, low cost and availability as a commodity. The ALD method is used with TMIn and O_3(ozone). In addition to ITO, other transparent conducting oxides can be prepared including, for example, doped ITO and tin zinc oxide.

3) ALD of Transparent Conducting Oxides using Synergistic Effect: We developed a method for the ALD of In_2O_3 that uses a combination of H_2O and O_2 as the oxygen source. These two molecules act synergistically to produce the surface chemistry necessary for the In_2O_3 ALD – either compound alone is insufficient. The advantage of this method over previous methods for In_2O_3 ALD using O_3 as the oxygen source is that H_2O and O2 are both stable, unlike O_3 that can decompose on surfaces. As a consequence, this synergistic ALD method allows highly porous

or high aspect ratio substrates to be coated with great precision. Such substrates are ideal for fabricating next generation, 3D photovoltaics. The synergistic In_2O_3 ALD of can be combined with existing processes for the ALD of SnO_2 to synthesize ITO, one of the highest performing transparent conducting oxides known, to serve as a transparent contact on 3D photovoltaics to improve their performance.

Instruments/Equipment

LSR (Large Substrate Reactor): The large substrate reactor was designed to coat up to 12”x18” substrates to scale-up ALD processes initially developed on the 1”x1” ALD tools used for exploratory studies in the Argonne ALD labs. The LSR is a cross-flow system that utilizes a kalrez o-ring seal for operation to ~250ºC, custom flow distributers on the precursor inlet and exhaust, and rod heaters for efficient heating and uniform temperature distribution. The LSR has used to scale up the synergistic ITO process that is currently being employed in our partnership with Bloo Solar, Inc.

Software

1) SMART (Simple Model for ALD Reaction and Transport): We developed a simple model to simulate the one-dimensional (1-D) reaction kinetics and transport of a chemical precursor during the thin film growth of an atomic layer deposition (ALD) condition in a circular tube. ALD has self-limiting surface reactions that permit homogeneous growth in high surface areas and nanostructured substrates. ALD is done under a vacuum and has two steps that include a pre-cursor application (and then a purging step) and then a cursor application (and then a purge). The problem faced in many instances is the high aspect ratio (length/diameter) of the substrate and it is a trial and error effort in getting the application times right so that the material can be transported along the entire length of the substrate. That is, what is the deposition time needed, what flow rates are needed, what is the pre-cursor/cursor reaction rates, etc. such that the total area of the substrate is coated. This software solves that problem and has been validated with data, for Al2O3 using water and trimethyl aluminum and will be extended to 3D geometries. Other pre-cursor/cursor ALD coatings have been tested. No other existing software can perform this analysis. There is a simple graphical user interface, and some examples to help users. The software is user friendly and can be run with confidence in 5-10 minutes. This program is intended to assist the ALD community in estimating process conditions for achieving uniform coverage, and is available free of charge on the Argonne ALD website. The model is web-based using a Java front end, and can run on any system with a Virtual Java Machine installed, including Windows, OSX, Linux/Unix operating systems. Run times are in seconds. The code is written in Python and Java.

2) SALMS (Simple ALD multiscale simulation): SALMS is a set of tools to carry out 3D simulations of thin film deposition under ALD conditions. SALMS takes as an input a finite set of parameters describing the nature of the ALD precursor-surface interaction and solves the time dependent process of precursor transport and thin film growth in reactors of arbitrary shape. Customization of SALMS allows the exploration of other relevant aspects of ALD process development, including the impact of purge times by allowing the visualization of the gas phase interaction of two sequentially dosed precursor species, as well as the multiscale simulation of

the coating of high aspect ratio features by linking feature and reactor length scales. Multiscale simulations are carried out through a new algorithm that takes advantage of the properties of self-limited processes and allows a fast coupling of feature and reactor length scales. This leads to multiscale simulations that are almost as fast as the simpler CFD reactor-scale simulations, in which the additional computational cost is a fixed overhead.

3) MachBall (Markov chain solver for ballistic transport with surface chemistry): Machball is a python package that simulates the transport of gas molecules inside a volume in presence of reacting surfaces under molecular flow. Machball can be regarded as a two component package: a) absmarkov is a python module that is a generic solver of absorbing Markov chain models, providing as an output the probabilistic outcome of the process, the average number of steps, and the average number of times that the system spends in each transient state, given any starting probability distribution. B) Machball uses absmarkov to simulate the transport of molecules inside volumes with reacting walls. Machball assumes that the interior walls of a volume can be divided into a finite number of disjoint sections, each of which is characterized by an arbitrary number of reaction pathways with a certain reaction probability. The transitions between different regions in the feature depend on the reemission model and the geometric shape of the volume, and they can be supplied by the user in the most general case. However, for a number of simple geometries and transport models, Machball can provide transition probabilities for the user. While Machball's main goal is to solve transport problems under molecular flow, absmarkov is a general module that could be applied to solve any user-defined Markov Chain model. These models are common in areas such as testing and reliability, queuing theory, economics, and finance. From this perspective, Machball can be regarded as an example of the application of absmarkov to a particular problem.

***Awards*:**
2012 R&D 100 Award, “Large Area Microchannel Plates”

2013 R&D 100 Award, “Nanocomposite Charge Drain Coatings”

Energy Systems Division
Argonne National Laboratory
9700 South Cass Avenue, Bldg. 362
Argonne, IL 60439

www.anl.gov

Argonne National Laboratory is a U.S. Department of Energy
laboratory managed by UChicago Argonne, LLC